Differential Laser Doppler Velocimeter With Enhanced Range for Small Wavelength Sensitivity by Using Cascaded Mach–Zehnder Interferometers

Koichi Maru, *Member, IEEE*, and Yusaku Fujii, *Member, IEEE*

***Abstract*—A differential laser Doppler velocimeter (LDV) with enhanced wavelength range for small wavelength sensitivity is proposed by using cascaded Mach–Zehnder interferometers (MZIs) for shifting the position of the beam at the input plane according to the wavelength. The cascaded MZI structures are used to enhance the position shift of the beam at the input plane compared with the use of single-stage MZIs. The gradual shift in the incident angle of the beam to the object is brought about with the combination of cascaded MZI structures, lenses and apertures. The simulation results indicate that the wavelength range for small wavelength sensitivity can be successfully enhanced by using two-stage cascaded MZI structures.**

***Index Terms*—Laser doppler velocimeter, interferometry, optical planar waveguides, precision measurement, wavelength sensitivity.**

I. Introduction

In research and industrial applications, laser Doppler velocimeters (LDVs) have been widely used to measure the velocity of a fluid flow or rigid object. The measurement by using a differential LDV has the advantage of contactless, small measuring volume giving excellent spatial resolution, and a linear response [1]–[4].

Using a semiconductor laser as a lightsource of an LDV is desirable to reduce the cost of equipment. However, typical inexpensive semiconductor lasers suffer from the problem of instability in lasing wavelength due mainly to the dependence on temperature. In conventional differential LDVs, a Doppler frequency shift at a monitoring point depends on the signal wavelength to be used. Hence, wavelength instability in semiconductor lasers causes measurement errors in the Doppler frequency shift.

To reduce the measurement error due to wavelength change, some studies have been reported [5]–[8] utilizing the change in the incident angle according to wavelength shift, such as a differential LDV using a diffractive grating [5]–[7] or arrayed waveguide gratings (AWGs) [8]. However, these types of the LDVs need complicated grating elements such as a diffractive grating or a planar waveguide grating. As a wavelength-insensitive LDV consisting of simpler optical elements, we have proposed the LDV that consists of single-stage Mach–Zehnder interferometers (MZIs), lenses and apertures, and proved a wavelength-insensitive operation [9]. The position shift of the beam induced by the MZI is converted into the shift in the incident angle to the measured point, and the aperture contributes to smoothing and continuously shifting the field distribution. In this structure, the wavelength range for small wavelength insensitivity is limited to several nanometers. It is desirable to enhance the wavelength range for small wavelength sensitivity in some cases, for example, when a cheap uncooled semiconductor laser is used as a lightsource.

In this paper, we propose a differential LDV with enhanced wavelength range for small wavelength sensitivity by using cascaded MZI structures for shifting the position of the beam at the input plane according to the wavelength. Cascaded MZI structures have been used for applications to optical communication such as multi/demultiplexers [10]–[12] or synchronized routers [13], [14]. In the proposed LDV, cascaded MZI structures are used to enhance the position shift of the beam at the input plane compared with the previous work using single-stage MZIs [9].

II. Principle

A. Structure

In a differential LDV, detected beat frequency, F_D, is expressed as [1], [3], [15]

$$F_D = \frac{2v_\perp \sin\psi}{\lambda} \tag{1}$$

where ψ is the incident angle of the beam to the object, $v_\perp$ is the velocity of the object perpendicular to the bisector of the angles of the incident beams to the object, and λ is the wavelength. From this equation, if ψ appropriately changes depending on λ, the wavelength-insensitive operation can be expected. When F_D is to be wavelength-insensitive around $\lambda = \lambda_0$, the derivative of F_D with respect to λ should be zero around $\lambda = \lambda_0$. From (1), this condition is expressed as

$$\left.\frac{d\psi}{d\lambda}\right|_{\lambda=\lambda_0} = \frac{\tan\psi_0}{\lambda_0} \tag{2}$$

where ψ_0 is the incident angle at $\lambda = \lambda_0$.

Fig. 1 illustrates the proposed wavelength-insensitive LDV using cascaded MZI structures. It consists of a laser, collimation optics, a power splitter, receiving optics, a photodetector (PD), and two sets of components, each of which consists of a mirror,

Manuscript received November 04, 2009; revised February 13, 2010; accepted March 21, 2010. Date of publication April 05, 2010; date of current version May 26, 2010. This work was supported in part by a research-aid fund of the Nakatani Foundation of Electronic Measuring Technology Advancement and Grant-in-Aid for Scientific Research (B) 21360196 (KAKENHI 21360196).

K. Maru and Y. Fujii are with the Department of Electronic Engineering, Gunma University, Gunma 376-8515, Japan (e-mail: maru@el.gunma-u.ac.jp; fujii@el.gunma-u.ac.jp).

Digital Object Identifier 10.1109/JLT.2010.2046880

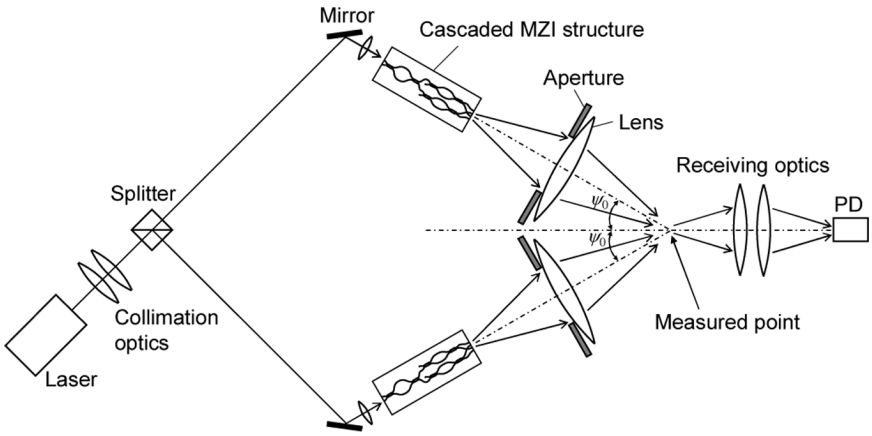

Fig. 1. Proposed wavelength-insensitive LDV using cascaded MZI structure.

a cascaded MZI structure, an aperture, and a lens close to the aperture. These two sets of the components having the same optical characteristics are symmetrically arranged. The input beam is split with a power splitter. Each beam is passing through the cascaded MZI structure. The ratio of the powers of the beams from output ports of the cascaded MZI structure changes according to the wavelength. The beam freely propagates, passes through the aperture and the lens, freely propagates again, and is incident to the measured point. The position shift of the beam at the output of the cascaded MZI structure is converted into shift in propagation angle at the measured point by the lens, and then, the incident angle ψ changes depending on the wavelength. The beams are scattered on the object at the measured point and detected by the PD as the beat of the light that depends on the Doppler shift due to the motion of the object.

To enhance the range in position shift according to wavelength compared with a single MZI, cascaded MZI structures are employed. Fig. 2 outlines the set of the components using a two-stage cascaded MZI structure. Signals with different wavelengths to the output of an $(l-1)$-th-stage MZI are demultiplexed with an l-th-stage MZI by setting the free spectral range of the l-th-stage MZI to twice that of the $(l-1)$-th-stage MZI. For the two-stage cascaded MZI structure, signals with four equally-spaced wavelengths $\lambda_1, \ldots, \lambda_4$ within one free spectral range are first divided with a first-stage MZI between the two groups λ_1, λ_3 and λ_2, λ_4, and next divided with second-stage MZIs into each signal. The lower port of the upper second-stage MZI and the upper port of the lower second-stage MZI should cross each other so that the four signals $\lambda_1, \ldots, \lambda_4$ are spatially arranged in this order at the input plane (i.e., at the output of the cascaded MZI structure). These output ports of the cascaded MZI structure are equally spaced with an interval d.

To obtain wavelength-insensitive operation, the field should be smoothed and continuously shifted at the output plane (i.e., around the measured point) as the change in the wavelength. The aperture contributes to smoothing and continuously shifting the field distribution at the output plane according to wavelength change as shown in Fig. 2. The aperture acts as a spatial filter for truncating a part of the diffraction pattern of the beams from the discrete ports of the cascaded MZI structure. Especially, when

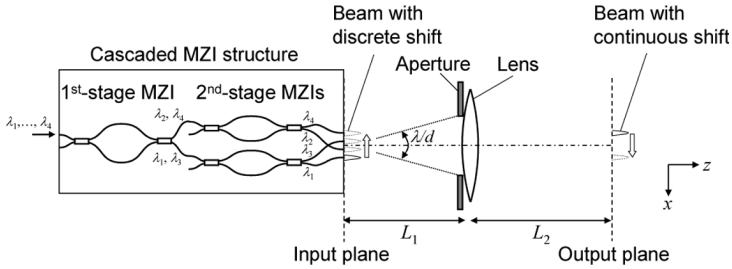

Fig. 2. Set of components consisting of two-stage cascaded MZI structure, aperture, and lens.

the spatial filter transmits just the pattern within one Brillouin zone determined by the arc subtended by the angle λ/d [16], [17], i.e., the zone covering just one fringe of the periodic pattern, the field distribution at the output plane is smoothed due to spatial band limitation.

The proposed structure can potentially be constructed as follows. First, the cascaded MZI structure is fabricated with planar lightwave circuit (PLC) technology [18]. There have been some reports [10], [11], [14] in which a cascaded MZI structure was fabricated by using silica waveguides. Second, each set of components consisting of the cascaded MZI structure, an aperture and a lens is submounted. Third, a laser, collimation optics, a splitter, mirrors and the submounts of the components are arranged so that the beams cross each other at the measured point. Here, the beam from the laser is coupled to the input waveguide of each cascaded MZI structure by using lenses. The focal length of the coupling lenses should be chosen according to the spot size of the beam and the dimension of the waveguide at the input of the cascaded MZI structure. Finally, receiving optics and a PD are arranged.

B. Paraxial Lens System

A set of optical components shown in Fig. 2 is modeled using paraxial approximation of a lens system with an aperture based on our previous work [9] to simulate the characteristics of the proposed structure. For simplicity, we treat one-dimensional case.

The transfer function for the m-th output port ($1 \le m \le M$) of a cascaded MZI structure with M output ports, $h_m(\lambda)$, is generally expressed as [12]

$$h_m(\lambda) = \frac{1}{M} D_M \left(\frac{\lambda_0 - \Delta\lambda}{\Delta\lambda_{\mathrm{FSR}}} + \frac{m-1}{M} + \varphi_1 \right) \times \exp\left[j(M-1)\pi \frac{\lambda_0 - \Delta\lambda}{\Delta\lambda_{\mathrm{FSR}}} + j\varphi_2 \right] \quad (3)$$

where $M = 2^L$ (L is the number of stages), λ_0 is the nominal wavelength, $\Delta\lambda$ is the wavelength shift from λ_0, $\Delta\lambda_{\mathrm{FSR}}$ is the free spectral range of the final-stage MZIs, φ_1 and φ_2 are the constant phases and $D_N(x)$ is the Dirichlet kernel defined as $D_N(x) = \sin(N\pi x)/\sin(\pi x)$ [19]. The beam from a single-mode waveguide is approximated as a Gaussian function. Let the field distribution of a normalized one-dimensional Gaussian beam from a waveguide at the input plane, $u_0(x)$, be

$$u_0(x) = \sqrt[4]{\frac{2}{\pi w_{\mathrm{in}}^2}} \exp\left[-\left(\frac{x}{w_{\mathrm{in}}} \right)^2 \right] \quad (4)$$

where w_{in} is the spot size. The total field distribution at the input plane, $u_1(x)$, is given by the superposition of M separated Gaussian beams, i.e.,

$$u_1(x) = \sum_{m=1}^{M} h_m(\lambda) u_0 \left(x + \left(m - \frac{M+1}{2} \right) d \right). \quad (5)$$

The Fourier transform of $u_1(x)$ is then given by

$$U_1(x) = \sqrt[4]{2\pi w_{\mathrm{in}}^2} \exp\left[-\left(\frac{k w_{\mathrm{in}} x}{2L_1} \right)^2 \right] \times \sum_{m=1}^{M} h_m(\lambda) \exp\left[j \frac{kdx}{L_1} \left(m - \frac{M+1}{2} \right) \right], \quad (6)$$

where $k = 2\pi/\Lambda$ is the wave number in the air and L_1 is the distance between the input plane and the aperture. Here, the Fourier transform of $f(x)$ is defined by

$$F(x) = \int_{-\infty}^{\infty} f(x_0) \exp\left(jk \frac{x x_0}{L_1} \right) dx_0. \quad (7)$$

The field distribution of the beam at the output plane, $u_2(x)$, is given by using paraxial approximation of a lens system [20] with an aperture as

$$u_2(x) = \frac{j \exp\left[-jk\left(\frac{x^2}{2L_2} + L_1 + L_2 \right) \right]}{\lambda^3 L_1^2 \sqrt{L_1 L_2}} P\left(\frac{L_1}{L_2} x \right) * G_2\left(\frac{L_1}{L_2} x \right) * \left[G_1\left(\frac{L_1}{L_2} x \right) U_1\left(\frac{L_1}{L_2} x \right) \right], \quad (8)$$

where L_2 is the distance between the lens and the output plane, and the functions $G_1(x)$ and $G_2(x)$, which represent parabolic phase change under Fresnel diffraction, are defined by

$$G_1(x) = \sqrt{\frac{\lambda L_1}{j}} \exp\left(jk \frac{x^2}{2L_1} \right), \quad (9)$$

$$G_2(x) = \sqrt{\frac{\lambda}{j\left(\frac{1}{L_2} - \frac{1}{f} \right)}} \exp\left[jk \frac{x^2}{2L_1^2 \left(\frac{1}{L_2} - \frac{1}{f} \right)} \right], \quad (10)$$

where f is the focal length of the lens near the aperture. $P(x)$ is the Fourier transform of the aperture function as

$$P(x) = \frac{2L_1 \sin \frac{kax}{L_1}}{kx} \quad (11)$$

where a is the half width of the aperture. The half width of the aperture that just covers one Brillouin zone, a_B, is determined as

$$a_B = \frac{L_1 \lambda}{2d}. \quad (12)$$

As a special case, when the output plane is set to the image plane defined by the thin-film equation and the distance between the aperture and the lens is negligible, the following relation holds between L_1 and L_2 [21]:

$$\frac{1}{f} = \frac{1}{L_1} + \frac{1}{L_2}. \quad (13)$$

III. Simulation Results and Discussion

The characteristics of the LDV is simulated by using the lens system model expressed as (8), assuming that two-stage cascaded MZI structures (i.e., $M = 4$) made from silica waveguides [18] are used. It is also assumed that the relative index difference between a core and cladding is 0.3%, the core width at the output of the MZI structures is 10 μm, and $d = 20$ μm. w_{in} is then assumed to be 4.74 μm under Gaussian approximation, derived from the approximated relation between the normalized core width and the spot size of the fundamental mode [22]. The nominal wavelength λ_0 is set to 1.3 μm to be used as an example of simulation. The aperture width $2a$ is set to the width just covering one Brillouin zone determined by (12). The position of the output plane is set to the image plane determined by (13).

Fig. 3 shows the contour plot of the calculated power distribution of the beam at the output plane for a two-stage cascaded MZI structure as a function of relative wavelength deviation $\Delta\lambda/\Delta\lambda_{\mathrm{FSR}}$. The power distributions are plotted for various aperture widths ($a/a_B = 0.5$, 0.75, 1.0, 1.25, 1.5, and without an aperture). Here, $f = 2$ mm and $L_1 = L_2 = 4$ mm. When a/a_B is larger than 1.0 (i.e., Fig. 3(d), (e) and (f)), the field at the output plane tends to be discretely shifted as the wavelength changes. When a/a_B is equal to or smaller than 1.0 (i.e., Fig. 3(a), (b), (c)), the field distribution at the output plane has only one peak and the position of the beam shifts continuously as the change of the wavelength. The smooth field distribution and continuous shift for the LDV with the aperture are due to the effect of spatial band limitation by the aperture. We should note that the field distribution is broadened when a/a_B is smaller than 1.0. It is because the reconstructed field at the output plane is excessively bandlimited. From the viewpoint of spatial resolution, smaller measurement volume is preferable. Hence, an a/a_B value of around 1.0 should be optimum in terms

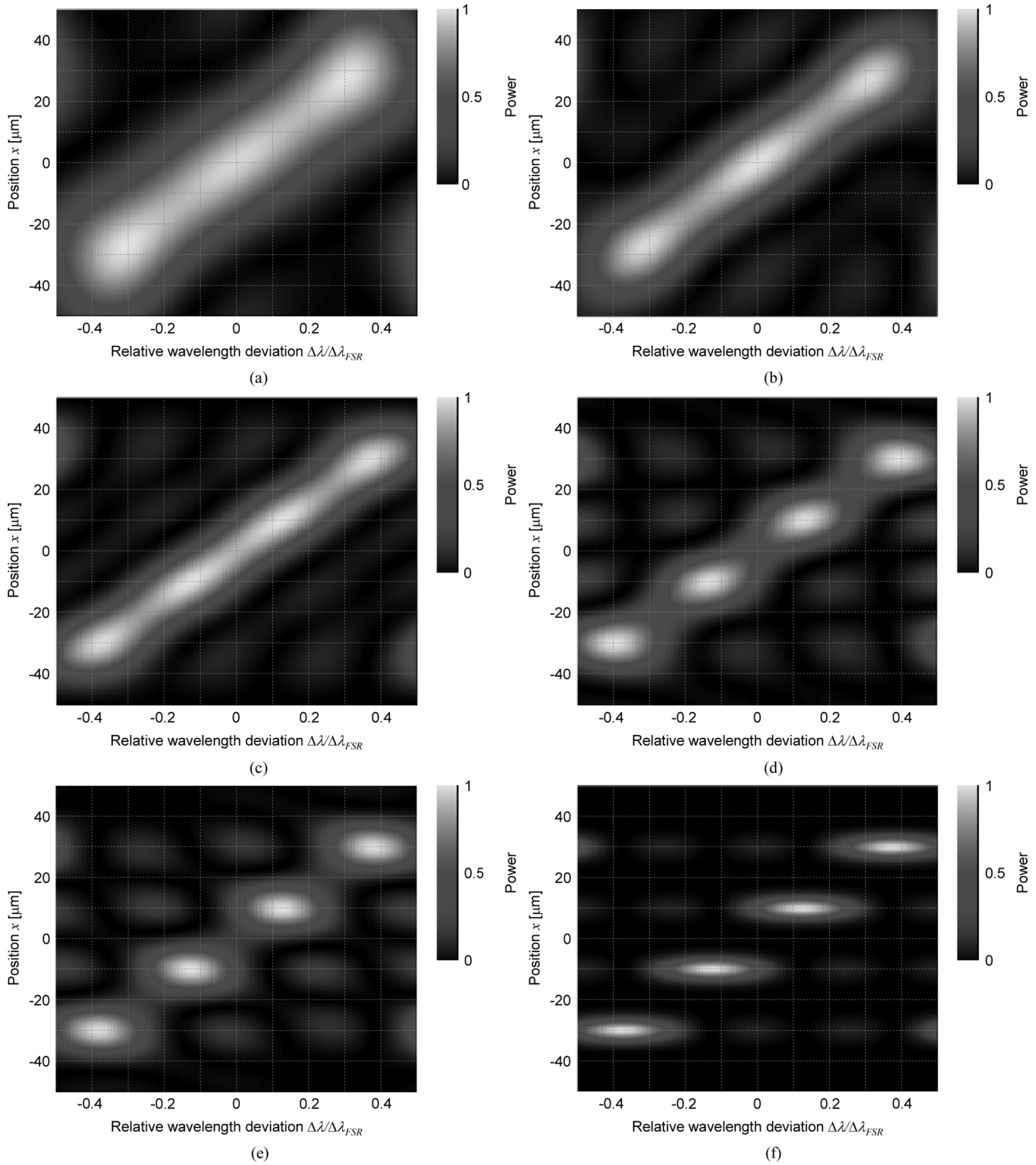

Fig. 3. Contour plot of calculated power distribution of beam at output plane as function of $\Delta\lambda/\Delta\lambda_{\mathrm{FSR}}$ for two-stage MZI structure. $f = 2$ mm and $L_1 = L_2 = 4$ mm. (a) $a/a_B = 0.5$, (b) $a/a_B = 0.75$, (c) $a/a_B = 1.0$, (d) $a/a_B = 1.25$, (e) $a/a_B = 1.5$, and (f) without aperture.

of smooth field distribution, continuous shift and small measurement volume. Hereafter, it is assumed that $a/a_B = 1.0$.

Fig. 4 plots the propagation angle at the output plane as a function of the relative wavelength deviation $\Delta\lambda/\Delta\lambda_{\mathrm{FSR}}$. Here, the propagation angle is defined by the angle between the direction of propagation and the z-axis. As well as the case for a two-stage cascaded MZI structure, the conventional case for a single-stage MZI (i.e., $M = 2$) with the same core width and d is also plotted in this Figure. The propagation angle of the beam changes as the change of the wavelength λ. It results from the conversion of the position shift of the beam at the input plane caused by wavelength shift into the shift in propagation angle

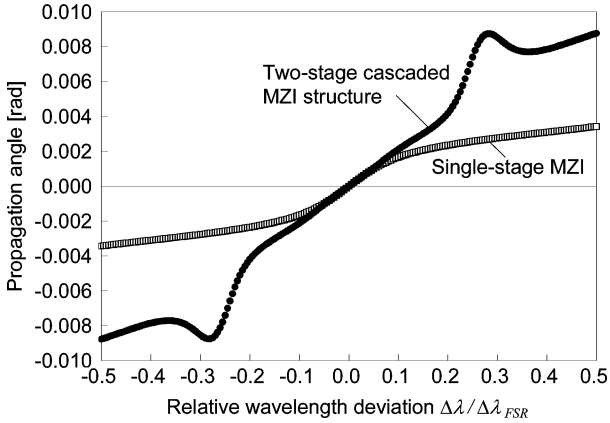

Fig. 4. Propagation angle at output plane as function of $\Delta\lambda/\Delta\lambda_{\rm FSR}$ for two-stage cascaded MZI structure ($M = 4$) and single-stage MZI ($M = 2$). $f = 2$ mm and $L_1 = L_2 = 4$ mm.

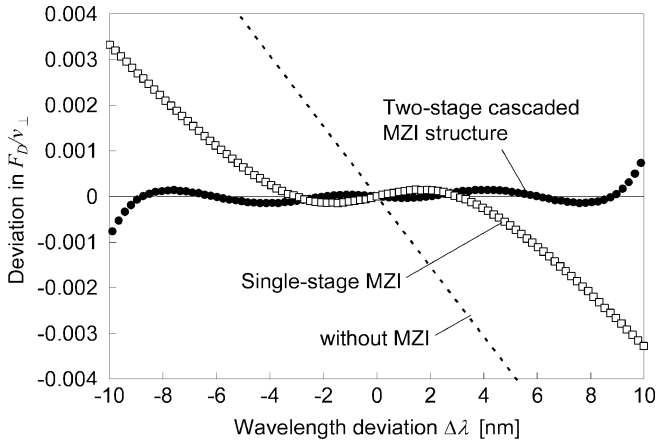

Fig. 5. Deviation in $F_D/v_\perp$ of LDV using two-stage cascaded MZI structures as function of $\Delta\lambda$. $\psi_0 = 30°$, $f = 2$ mm, and $L_1 = L_2 = 4$ mm. The deviation for conventional LDV without MZIs and conventional LDV using single-stage MZIs are also plotted in this figure.

by the lens. The wavelength range in which change in propagation angle is almost linear can be increased to about ± 0.2 of $\Delta\lambda/\Delta\lambda_{\rm FSR}$ by using a two-stage cascaded MZI structure, whereas the range is about ± 0.1 of $\Delta\lambda/\Delta\lambda_{\rm FSR}$ for the conventional case using a single-stage MZI. The range in propagation angle is also increased from about ± 0.0015 rad for a single-stage MZI to about ± 0.004 rad for a two-stage cascaded MZI structure. When the beam shifts between the marginal output ports for a two-stage cascaded MZI structure, the wavelength shifts from -0.375 to $+0.375$ of $\Delta\lambda/\Delta\lambda_{\rm FSR}$ with a position shift from $-1.5d$ to $+1.5d$. On the other hand, the wavelength shift is from -0.25 to $+0.25$ of $\Delta\lambda/\Delta\lambda_{\rm FSR}$ with a position shift from $-0.5d$ to $+0.5d$ for the conventional case. This enhancement in the wavelength shift and position shift leads to enhancing the range for almost linear change.

$\Delta\lambda_{\rm FSR}$ for wavelength-insensitive operation should be derived as a parameter for the MZI structure, once the incident angle ψ_0 is fixed. From Fig. 4, the increment of the incident angle ψ with respect to $\Delta\lambda/\Delta\lambda_{\rm FSR}$ is derived as 0.0204 rad around $\lambda = \lambda_0$. $\Delta\lambda_{\rm FSR}$ is then derived so that the relation (2) approximately satisfies after ψ_0 is fixed. When ψ_0 is set to 30° for example, $\Delta\lambda_{\rm FSR}$ should be set to 46.0 nm.

Fig. 5 plots the deviation in $F_D/v_\perp$ of an LDV using two-stage cascaded MZI structures due to the wavelength deviation $\Delta\lambda = \lambda - \lambda_0$ calculated by using (1) for $\psi_0 = 30°, f = 2$ mm, and $L_1 = L_2 = 4$ mm. The deviation in $F_D/v_\perp$ is defined as $[F_D/v_\perp - (F_D/v_\perp)|_{\lambda=\lambda 0}]/(F_D/v_\perp)|_{\lambda=\lambda 0}$. For comparison, the deviations for a conventional LDV without MZIs and a conventional LDV using single-stage MZIs are also shown in Fig. 5. The wavelength range with small deviation in $F_D/v_\perp$ can be increased by using cascaded MZI structures. The wavelength range for small deviation in $F_D/v_\perp$ (within $\pm 1.5 \times 10^{-4}$) is ± 9.1 nm for the LDV using two-stage cascaded MZI structures, whereas the range is ± 3.6 nm for the conventional LDV using single-stage MZIs.

When allowable deviation in $F_D/v_\perp$ is once determined, the wavelength range for the allowable deviation in $F_D/v_\perp$ can be maximized by optimizing $\Delta\lambda_{\rm FSR}$ because the increment of $F_D/v_\perp$ with respect to λ is determined by $\Delta\lambda_{\rm FSR}$. Fig. 6 shows the relation between allowable deviation in $F_D/v_\perp$ and half

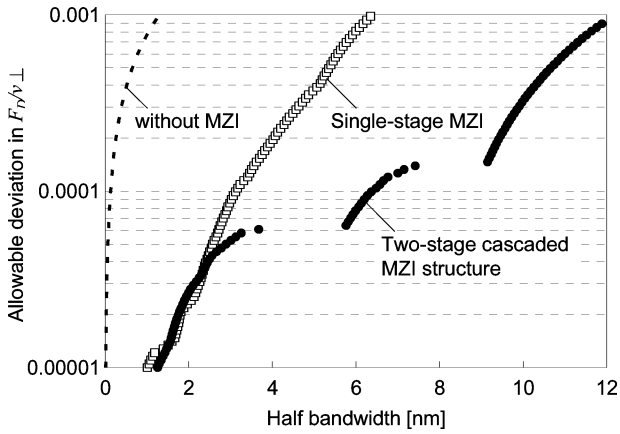

Fig. 6. Relation between allowable deviation in $F_D/v_\perp$ and half bandwidth. $\psi_0 = 30°$, $f = 2$ mm, and $L_1 = L_2 = 4$ mm.

bandwidth. The half bandwidth is defined as the half of the full wavelength range within which the absolute value of the deviation in $F_D/v_\perp$ is below the allowable deviation. It is found that the half bandwidth is wider for the LDV using two-stage cascaded MZI structures when the absolute value of the deviation in $F_D/v_\perp$ of larger than 5×10^{-5} is allowable. When the allowable deviation is larger than 6.4×10^{-5}, the bandwidth for the two-stage cascaded MZI structure becomes larger than twice that for the single-stage MZI. The half bandwidth for the two-stage cascaded MZI structure has two discontinuities caused by some slight nonlinear changes in the wavelength dependence of propagation angle.

As well as the paraxial lens system model expressed as (8), we simulated the field distribution by the beam propagation method (BPM) as a conventional method for simulating beam propagation to verify the simulation result from the lens system model. We used commercially available software (BEAMPROP ver.8.1, RSoft Inc.) for the BPM simulation. We compared the numerical result from the lens system model expressed as (8) with that from simulation using the BPM. We only simulated the free propagation region between the input plane and the output plane including the lens and the aperture with the BPM, whereas

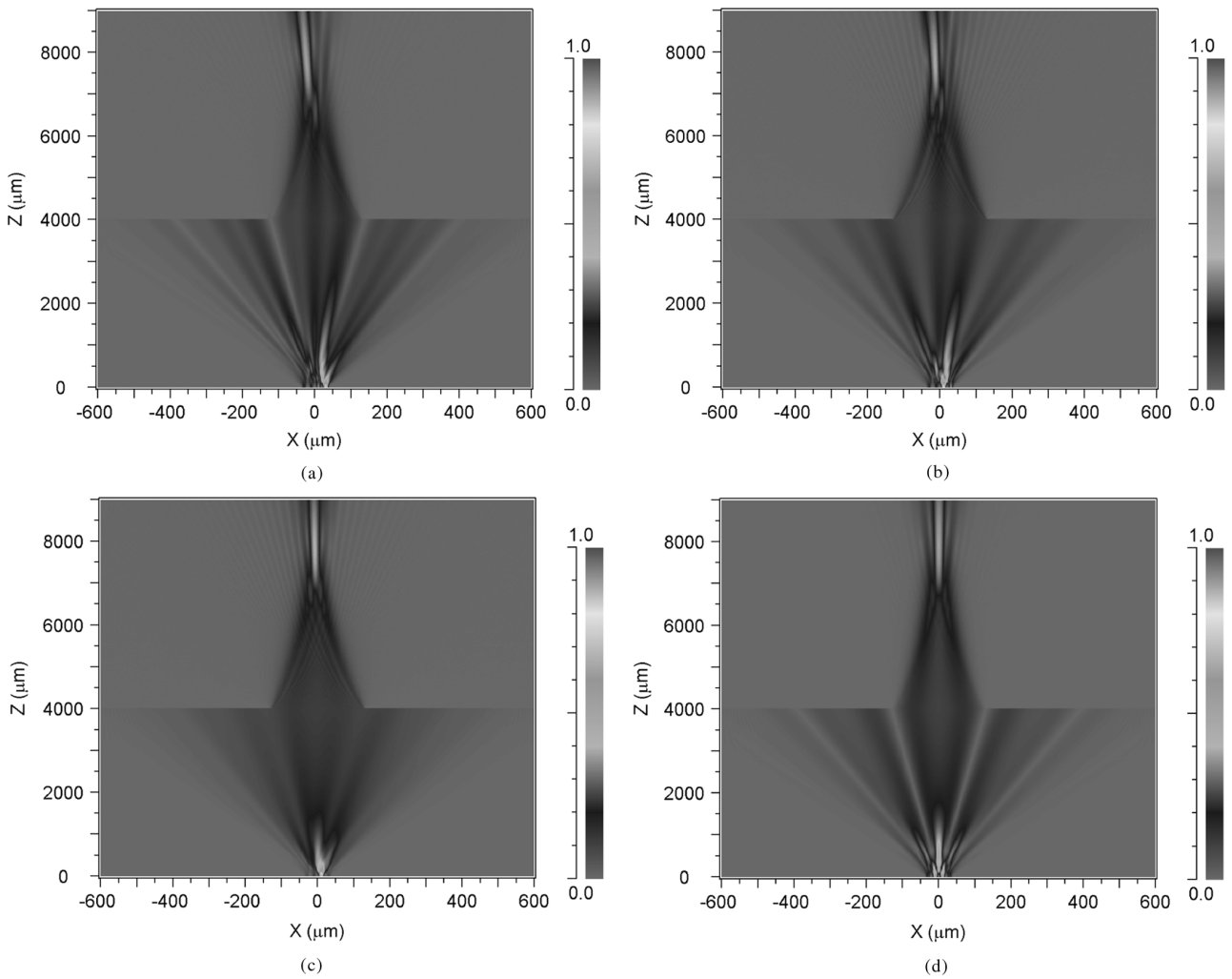

Fig. 7. Contour plot of field amplitude of diffraction pattern from input plane to around the output plane by BPM. $d = 20\,\mu$m, $w_{\rm in} = 4.74\,\mu$m, $f = 2$ mm, $L_1 = L_2 = 4$ mm and $a/a_B = 1.0$. (a) $\Delta\lambda/\Delta\lambda_{\rm FSR} = -0.3$, (b) $\Delta\lambda/\Delta\lambda_{\rm FSR} = -0.2$, (c) $\Delta\lambda/\Delta\lambda_{\rm FSR} = -0.1$, (d) $\Delta\lambda/\Delta\lambda_{\rm FSR} = 0$. Here, the input plane is at $z = 0$, the lens and the aperture are at $z = 4$ mm, and the output plane is at $z = 8$ mm.

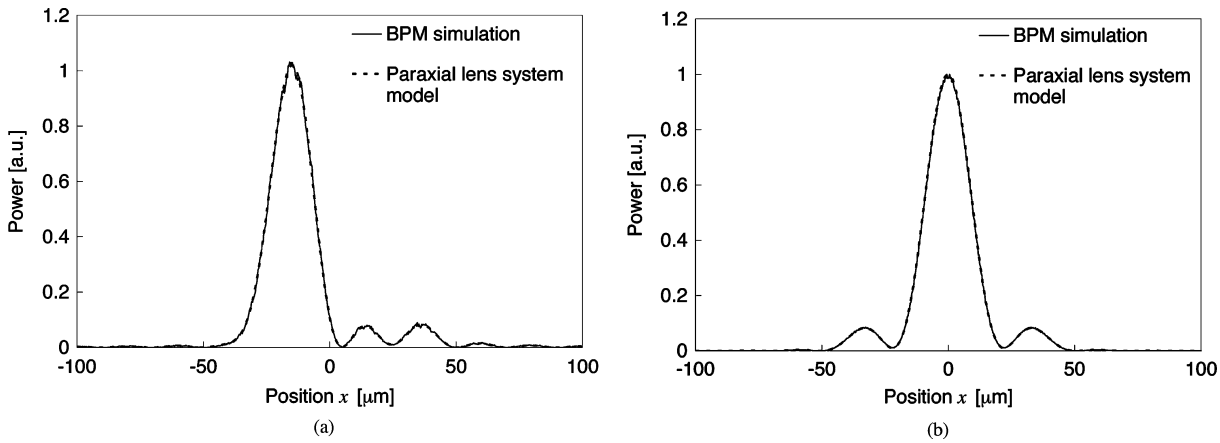

Fig. 8. Calculated power distribution of beam at output plane for BPM simulation and paraxial lens system model. $f = 2$ mm, $L_1 = L_2 = 4$ mm and $a/a_B = 1.0$. (a) $\Delta\lambda/\Delta\lambda_{\rm FSR} = -0.2$, (b) $\Delta\lambda/\Delta\lambda_{\rm FSR} = 0$.

the input amplitudes induced by a cascaded MZI structure were analytically given by (3) for $M = 4$.

Fig. 7 shows the contour plot of the field amplitude of the diffraction pattern from the input plane (i.e., the output of the cascaded MZI structure) to around the output plane by 2-D BPM simulation. It is assumed that $d = 20\,\mu$m, $w_{\rm in} = 4.74\,\mu$m, $f = 2$ mm, $L_1 = L_2 = 4$ mm and $a/a_B = 1.0$. The diffraction pattern reveals that the diffracted beam outside the central

Brillouin zone is screened by the aperture. Consequently, the field distribution has a single main peak around the output plane ($z = 8$ mm) even when the power splits mainly two output ports of the cascaded MZI structure. This result clearly indicates the effect of the band limitation by the aperture. Moreover, the shifts in the direction and the position of the beam around the output plane depending on the wavelength are appeared in the BPM simulation as well as the lens system model. It indicates that the wavelength sensitivity can be reduced by utilizing these shifts.

Fig. 8 plots the calculated power distribution of the beam at the output plane for the BPM simulation and the paraxial lens system model for $\Delta\lambda/\Delta\lambda_{\mathrm{FSR}} = -0.2$ and 0. The power distribution given by the lens system model agreed well with that given by the BPM simulation. This agreement indicates that the lens system model derived in Section II.B can be used to analyze the proposed LDV effectively.

IV. Conclusion

A differential laser Doppler velocimeter (LDV) with enhanced wavelength range for small wavelength sensitivity has been proposed by employing cascaded MZI structures for shifting the position of the beam at the input plane according to the wavelength. The cascaded MZI structures are used to enhance the position shift of the beam at the input plane. As a result of the simulation using a model of a lens system with an aperture, we found that the wavelength range for small wavelength sensitivity can be enhanced by using two-cascaded MZI structures. The wavelength range for small deviation in $F_D/v_\perp$ (within $\pm 1.5 \times 10^{-4}$) can be increased to ± 9.1 nm for the LDV using two-stage cascaded MZI structures, whereas the range is ± 3.6 nm for the conventional LDV using single-stage MZIs. It would be useful for low-cost and precise velocity measurement in many researches and industries.

References

[1] A. L. Duff, G. Plantier, J.-C. Valière, and T. Bosch, "Analog sensor design proposal for laser Doppler velocimetry," *IEEE J. Sens.*, vol. 4, no. 2, pp. 257–261, Apr. 2004.

[2] M. Haruna, K. Kasazumi, and H. Nishihara, "Integrated-optic differential laser Doppler velocimeter with a micro Fresnel lens array," in *Proc. Conf. Integ. Guided-Wave Opt. (IGWO'89)*, 1989, MBB6.

[3] T. Ito, R. Sawada, and E. Higurashi, "Integrated microlaser Doppler velocimeter," *J. Lightw. Technol.*, vol. 17, no. 1, pp. 30–34, Jan. 1999.

[4] J. W. Foreman, E. W. George, J. L. Jetton, R. D. Lewis, J. R. Thornton, and H. J. Watson, "8C2-fluid flow measurements with a laser Doppler velocimeter," *J. Quantum Electron.*, vol. QE-2, no. 8, pp. 260–266, Aug. 1966.

[5] J. Schmidt, R. Volkel, W. Stork, J. T. Sheridan, J. Schwider, and N. Steibl, "Diffractive beam splitter for laser Doppler velocimetry," *Opt. Lett.*, vol. 17, no. 17, pp. 1240–1242, Sep. 1992.

[6] R. Sawada, K. Hane, and E. Higurashi, *Optical Micro Electro Mechanical Systems* (in Japanese). Tokyo: Ohmsha, 2002, sec. 5.2.

[7] H.-E. Albrecht, M. Borys, N. Damaschke, and C. Tropea, *Laser Doppler and Phase Doppler Measurement Techniques*. : Springer—Verlag Berlin Heidelberg, 2003, sec. Section 7.2.2.

[8] K. Maru and Y. Fujii, "Integrated wavelength-insensitive differential laser Doppler velocimeter using planar lightwave circuit," *J. Lightw. Technol.*, vol. 27, no. 22, pp. 5078–5083, Nov. 2009.

[9] K. Maru and Y. Fujii, "Wavelength-insensitive laser Doppler velocimeter using beam position shift induced by Mach–Zehnder interferometers," *Opt. Exp.*, vol. 17, no. 20, pp. 17441–17449, Sep. 2009.

[10] N. Takato, K. Jinguji, M. Yasu, H. Toba, and M. Kawachi, "Silica-based single-mode waveguides on silicon and their application to guided-wave optical interferometers," *J. Lightw. Technol.*, vol. 6, no. 6, pp. 1003–1010, Jun. 1988.

[11] B. H. Verbeek, C. H. Henry, N. A. Olsson, K. J. Orlowsky, R. F. Kazarinov, and B. H. Johnson, "Integrated four-channel Mach–Zehnder multi/demultiplexer fabricated with phosphorous doped SiO_2 waveguides on Si," *J. Lightw. Technol.*, vol. 6, no. 6, pp. 1011–1015, Jun. 1988.

[12] C. K. Madsen and J. H. Zhao, *Optical Filter Design and Analysis*. New York: Wiley, 1999, ch. Chap. 3.

[13] K. Maru, T. Mizumoto, and H. Uetsuka, "Modeling of multi-input arrayed waveguide grating and its application to design of flat-passband response using cascaded Mach–Zehnder interferometers," *J. Lightw. Technol.*, vol. 25, no. 2, pp. 544–555, Feb. 2007.

[14] K. Maru, T. Mizumoto, and H. Uetsuka, "Demonstration of flat-passband multi/demultiplexer using multi-input arrayed waveguide grating combined with cascaded Mach–Zehnder interferometers," *J. Lightw. Technol.*, vol. 25, no. 8, pp. 2187–2197, Aug. 2007.

[15] H.-E. Albrecht, M. Borys, N. Damaschke, and C. Tropea, *Laser Doppler and Phase Doppler Measurement Techniques*. New York: Springer, 2003, sec. 2.1.

[16] C. R. Doerr, M. Cappuzzo, E. Laskowski, A. Paunescu, L. Gomez, L. W. Stulz, and J. Gates, "Dynamic wavelength equalizer in silica using the single-filtered-arm interferometer," *IEEE Photon. Technol. Lett.*, vol. 11, no. 5, pp. 581–583, May 1999.

[17] I. Kaminow and T. Li, *Optical Fiber Telecommunications IVA*. San Diego, CA: Academic, 2002, pp. 424–427.

[18] M. Kawachi, "Silica waveguides on silicon and their application to integrated-optic components," *Opt. Quantum Electron.*, vol. 22, no. 5, pp. 391–416, 1990.

[19] H. Dym and H. P. McKean, *Fourier Series and Integrals*. New York: Academic, 1972, ch. Chap. 1, pp. 31–32.

[20] J. W. Goodman, *Introduction to Fourier Optics*. San Francisco, CA: McGraw-Hill, 1968, ch. Chap. 4–5.

[21] J. W. Goodman, *Introduction to Fourier Optics*. San Francisco, CA: McGraw-Hill, 1968, p. 94.

[22] D. Botez and M. Ettenberg, "Beamwidth approximations for the fundamental mode in symmetric double-heterojunction lasers," *J. Quantum Electron.*, vol. QE-14, no. 11, pp. 827–830, 1978.

Koichi Maru (M'07) was born in Chiba, Japan, in 1972. He received the B.E. degree in electrical and electronic engineering, M.E. degree in physical electronics, and Ph.D. degree in electrical and electronic engineering from Tokyo Institute of Technology, Tokyo, Japan, in 1995, 1997, and 2007, respectively.

He worked in Hitachi Cable, Ltd., Ibaraki, Japan, from 1997 to 2008, where he was engaged in research and development on optical waveguide devices. Since 2008, he has been an Assistant Professor with the Department of Electronic Engineering, Faculty of Engineering, Gunma University, Japan. His research has been concerned mainly with Optical measurement and instrumentation engineering, planar lightwave circuits, and optical filtering devices.

He is a member of the Institute of Electronics, Information and Communication Engineers (IEICE) of Japan.

Yusaku Fujii (M'00) was born in Tokyo, Japan, in 1965. He received the B.E., M.E. and Ph.D. degrees from Tokyo University, Tokyo, Japan, in 1989, 1991 and 2001, respectively.

In 1991, he joined the Kawasaki Steel Corp. In 1995, he moved to the National Research Laboratory of Metrology (NRLM), Tsukuba, Japan, where he had studied for the replacement of the kilogram using the superconducting magnetic levitation. In 2002, he moved to Gunma University, Kiryu, Japan, where has invented and studied for the Levitation Mass Method (LMM) as a precision force measuring method.